Unsteady tidal turbine blade loading: an analytical approach

Unsteady Tidal Turbine Blade Loading; an Analytical Approach

Gabriel Scarlett, Ignazio Maria Viola*
Institute for Energy Systems, School of Engineering, University of Edinburgh, UK

Summary: A model utilising linear 2D analytical theory is used to quantify the unsteady loading on tidal turbine blades due to the combined effects of waves and turbulence with shear and tower shadow. Initial results show that unsteady loads are mostly dominated by low frequency turbulence and waves, but if pitch control is employed loads are reduced by three orders of magnitude.

Introduction

The translation of a tidal turbine blade through waves, turbulence, shear and tower shadow introduces a time dependent angle of attack (α). For small harmonic oscillations in fully attached flow the solution to the unsteady lift coefficient C_L is given by Theodorsen as added mass and circulatory components [1]. The former accounts for flow acceleration effects, and the latter for circulation around the foil and shed vorticity in the wake introducing a time delay and amplitude reduction from the quasi-static loads. Loewy adapted the model for a rotor in hover to account for the effects of neighbouring and returning wakes on the unsteady loads [2]. Recent research has shown that attached unsteady loads may exceed steady loads by up to 15% [3], but has been confined to axial perturbations caused by waves and turbulence [3], or waves and yaw misalignment [4]. In order to further aid the design process a model is introduced which incorporates turbulent perturbations in all three coordinates, wave induced velocities in the axial (x), and vertical (z) directions, as well as the velocity deficit in x, and induced velocity in y, due to the presence of a tower structure.

Method

A three bladed 18 m diameter rotor located in a channel 45 m in depth and operating at the optimum tip speed ratio of 4.5, is considered [5]. Tests are carried out at the mid-section where the profile takes that of a NACA $63-439$, where the chord length is 1.45 m, and the pitch is 13.5°. The zero lift and static stall angles were determined using Xfoil [6]. Four inline waves were tested with frequencies $\boldsymbol{f_w} = (0.13, 0.18, 0.29, 0.67)$ Hz, respective heights $\boldsymbol{H_w} = (3.25,\ 1.75, 0.75, 0.25)$ m, and probability occurrences $\boldsymbol{P_w} = (\ 0.07, 5.83, 27.16, 7.14)$. These were selected from a MET office data set of measurements from the Pentland Firth [7]. Wave particle velocities are determined in the x, and z coordinates using Stokes second-order wave theory. Turbulence is simplified by assuming it comprises of four frequency constituents $\boldsymbol{f_t} = (0.01, 0.1, 1, 4)$ Hz, with amplitudes matched respectively to the following kinetic energies, measured in The Puget Sound [8], in x, y and z coordinates: $\boldsymbol{Ek_x} = (1.2\times10^{-1},\ 1.15\times10^{-2}, 1.4\times10^{-4}, 1.1\times10^{-4})$ m^{2}s^{-2}, $\boldsymbol{Ek_y} = (1.1\times10^{-2}, 1.8\times10^{-3}, 1.4\times10^{-4}, 1.4\times10^{-5})$ m^{2}s^{-2}, $\boldsymbol{Ek_z} = \boldsymbol{Ek_y}$. Turbulent intensities of 12%, 9% and 7% in the x, y, and z coordinates, respectively, were selected from a flow characterisation study carried out at The Sound of Islay [9]. The shear profile is assumed to agree with the 1/7th power law where the mean current at the hub is 2 ms^{-1} at a depth of 20 m. The velocity deficit in x, and induced velocity in y caused by the presence of a 2 m diameter tower, 5 m downstream of the rotor are determined using a potential flow model. For each test an α history is formed, as shown in Fig. 1, where time (t) is non-dimensioned by the rotational period (T_{rot}). The amplitude and peak frequency are then determined in order to form a harmonic angle of attack (α_h) signal, so as to be introduced into the theories of Theodorsen and Loewy to determine C_L (Fig. 2).

Results

The amplitude load response ΔC_L for each individual frequency component (f) non-dimensioned by the rotational frequency (f_{rot}), is shown in Fig. 3. These results are in qualitative agreement with ref. [10]. The greatest load fluctuations are caused by low frequency turbulence, associated with channel scale eddies greater than 100 m, and large amplitude waves. Figure 4 shows the effect of each wave combined with all other forcing frequencies (turbulence, shear, tower shadow). The lowest frequency wave leads to the largest combined ΔC_L. Figure 1 shows the α history for this case over 20 rotations, and Fig. 2 illustrates the resulting C_L. Under this operating condition dynamic stall does not occur because the stall angle, which is greater than 20°, is not exceeded. Clearly at lower current velocities and closer to the root, separation might occur. With higher frequency waves,

* Corresponding author.
Email address: I.M.Viola@ed.ac.uk

the dominating combined effect on ΔC_L is low frequency turbulence. Interestingly, if pitch control was to be adopted so as to filter every frequency up to twice f_{rot}, ΔC_L would decrease by three orders of magnitude.

Conclusions

The combination of low frequency turbulence and +3 m high waves lead to maximum ΔC_L. However, load fluctuations due to relatively large waves (~2 m), shear layer and tower shadow are negligible compared to those due to low frequency turbulence. Load fluctuations can be reduced by three orders of magnitude using pitch control at $2\times f_{rot}$. Further research is ongoing to determine the effects over a broader range of conditions as well as the effects of yaw misalignment, site specific shear, and flow separation.

Acknowledgements:

This work was supported by the Physical Sciences Research Council [grant number EP/M508032/1].

References:

[1] Theodorsen, T. (1935). "General theory of aerodynamic instability and the mechanism of flutter," NACA Technical Report No. 496.
[2] Loewy, R.G. (1957). "A two-dimensional approximation to the unsteady aerodynamics of rotary wings," J. Aeronaut. Sci, 24 (2): 81-92.
[3] Milne, I.A., Day, A.H. Sharma, R.N. and Flay, R.G.J. (2015). "Blade loading on tidal turbines for uniform unsteady flow", Renewable Energy, 77:338-350.
[4] McNae, D. M. (2013) "Unsteady hydrodynamics of tidal stream turbines". PhD thesis. Imperial College London.
[5] Gretton, G.J., and Ingram, D.M., (2011), "Development of a computational fluid dynamics model for a horizontal axis tidal current turbine", PerAWaT, MA1003, WG3 WP5 D1.
[6] Drela, M. (1989). "XFOIL: An analysis and design system for low Reynolds number airfoils". In Low Reynolds number aerodynamics (pp. 1-12).
[7] McCann, G. N., Hitchcock, S., and Lane, S. (2008). "Implications of site-specific conditions on the prediction of loading and power performance of a tidal stream device", In ICOE 2008, Brest.
[8] Thomson, J., Polagye, B., Durgesh, V., and Richmond, M. C. (2012). "Measurements of turbulence at two tidal energy sites in The Puget sound, WA". J., Oceanic Eng., 37(3), 363 - 374.
[9] Milne, I. A., Sharma, R.N., Flay, R. G. J., and Bickerton, S. (2011). "Characteristics of the onset flow turbulence at a tidal-stream power site", In EWTEC 2011.
[10] Sequeira, C.L. and Miller, R.J., 2014, September. "Unsteady gust response of tidal stream turbines. In IEEE/MTS OCEANS'14, St. John's.

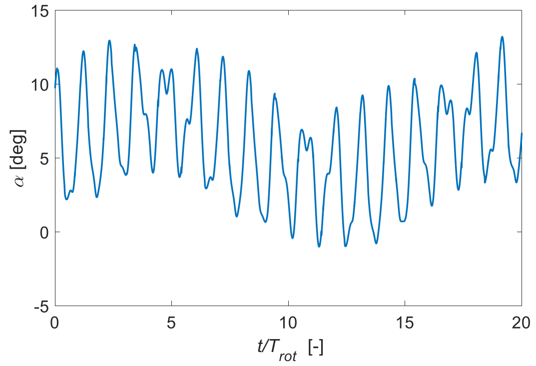

Fig. 1. Angle of attack fluctuations

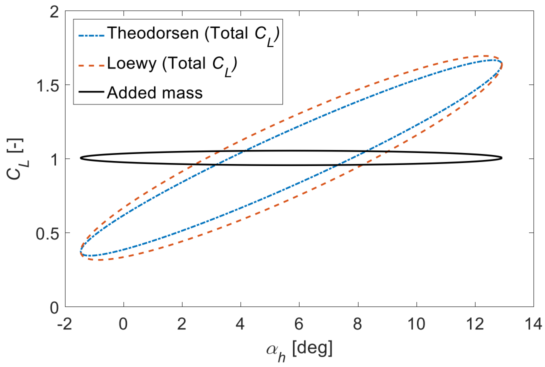

Fig. 2. Unsteady lift coefficient history

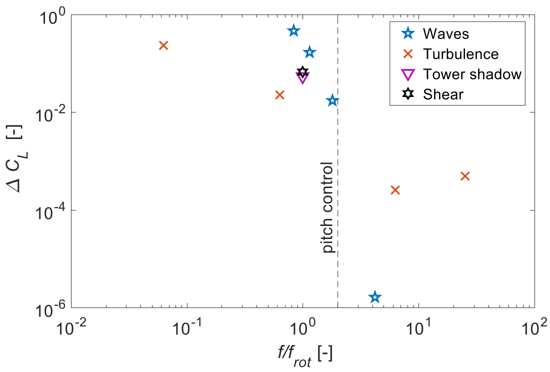

Fig. 3. Individual load effect

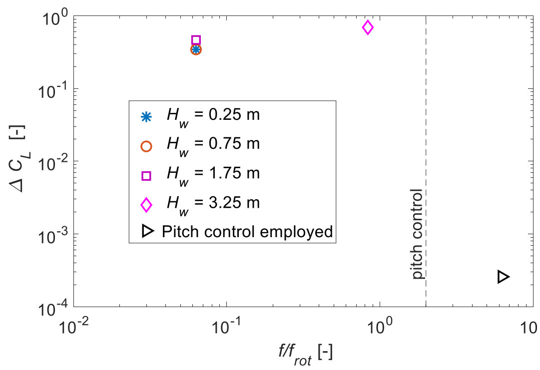

Fig. 4. Combined load response